Seventh Framework Programme

Theme 6

Environment

Project: 603864 – HELIX

Full project title:

High-**E**nd c**L**imate **I**mpacts and e**X**tremes

Deliverable: 3.1

Documentation of changes in climate variability and extremes simulated by the HELIX AGCMs at the 3 SWLs and comparison to changes in equivalent SST/SIC low-resolution CMIP5 projections

Version 1.0

Original Due date of deliverable: 30/04/2016

Actual date of submission: 31/01/2017

Delay approved by Project Officer

Documentation of changes in climate variability and extremes simulated by the HELIX AGCMs at the 3 SWLs and comparison to changes in equivalent SST/SIC low-resolution CMIP5 projections

January

2017

Documentation of changes in climate variability and extremes simulated by the HELIX AGCMs at the 3 SWLs and comparison in equivalent SST/SIC low-resolution CMIP5 projections

Klaus Wyser,Gustav Strandberg (SMHI)
John Caesar, Laila Gohar (MetOffice)

1 Introduction

The on-going advancement of computer hardware and information technology has created new opportunities for climate modeling. Climate models have become more complex with increased spatial resolution and better representation of physical processes. The frontiers of climate modeling are being pushed to new limits which has greatly improved our understanding of the climate system, processes, sensitivities and feedbacks, and which has improved our possibility to better simulate the climate and its anticipated changes in the future.

Several studies in the past have addressed the question about the benefits of higher model resolution. Among other effects a positive impact was found in the representation of atmospheric blockings (Jung et al. 2012, Berckmans et al. 2013, Dawson and Palmer 2014), precipitation (Chan et al. 2013, Van Haren et al. 2015), ocean circulation (Winton et al. 2014) or tropical cyclones (Murakami et al. 2015). An important impact of higher model resolution is a change in the drivers of the hydrological cycle (Demory et al. 2014) which is an important aspect of climate models when it comes to their ability to realistically simulate extreme precipitation events, river discharges or extreme soil moisture conditions. A good representation of the hydrological cycle is essential for the climate impact modeling and therefore we expect substantial benefits from higher spatial resolution.

The EU FP7 HELIX project aims at making projections of global impacts under future climate change, and to make these projections as useful as possible we chose models with higher resolution than the CMIP5 models to benefit from the advantages of higher resolution. Also, in HELIX we wanted to cover as much of the range of possible regional climate changes as we could within limited computing resources. We therefore decided to use atmosphere-only models that were forced with SST and sea-ice concentrations (SIC) from existing CMIP5 models. Prescribing SST and SIC allow our results to be easily comparable with other work by the wider climate science community, and in particular with the climate and climate change in the forcing CMIP5 models to assess the benefits of higher resolution. Furthermore, we also look in more detail at the impact of increasing resolution in one particular model.

The CMIP5 simulations were typically done with spatial resolutions of at least 200km. Here we use two climate models of the next generation with horizontal resolution of 30-60 km that will be used in upcoming CMIP6 experiments. These model versions not only feature higher resolution than their predecessors but also upgraded dynamics and parameterisations. To better understand the role of higher resolution we therefore split this study into two parts with the first part addressing the impact from higher resolution compared to CMIP5 models, and the second part looking at the impact of higher resolution if the same model is used with two different resolutions. The geographical focus of the evaluation is on the HELIX target regions of Europe, northern sub-Saharan Africa and South Asia. The effects from higher resolution are studied at different warming levels to see if increased resolution plays a similar role in changing climate compared to present-day.

2 High-resolution models

2.1 EC-EARTH3

The EC-EARTH3 model is developed jointly by the EC-EARTH consortium that comprises a number of European Met Services and research institutes (http://www.ec-earth.org). The EC-EARTH3 model v3.1 is an updated version of EC-EARTH v2.3 that was used for CMIP5 (Hazeleger et al. 2012 and Hazeleger et al. 2013).

The atmosphere module in EC-EARTH3 is based on IFS cy36r4 that is also used in the seasonal prediction system S4 at ECMWF (Molteni et al. 2011). The main differences to v2.3 are the introduction of the McRad scheme for a better representation of the interaction between radiation and subgrid clouds (Morcrette et al. 2008), and an entirely new microphysics with 5 prognostic classes of hydrometeors (Forbes et al. 2011). These two changes, in combination with an updated convection scheme have helped to greatly improve the representation of tropical precipitation. In addition to these updates a new humidity conservation was added to the EC-EARTH3 model. The humidity conservation has been backported from a later cycle of the IFS model to address the spurious sources and sinks of humidity that have been identified (Diamantakis and Flemming 2013).

The standard resolution of the atmosphere in EC-EARTH3 increased from T159 in CMIP5 to T255 (planned for CMIP6). For the simulations for the HELIX project the high-resolution version of the model (EC-EARTH3-HR) was used with T511 which corresponds to 0.35 deg nominal horizontal resolution (~40 km). The vertical resolution increased from 62 to 91 levels with a higher model top and most of the new levels added in the stratosphere.

Version 3.1 of the EC-EARTH model lies in the transition from the CMIP5 model towards the CMIP6 model. Many features have already been updated or added in v3.1, yet there are more changes expected for EC-EARTH3 before the CMIP6 simulations will start (expected in 2017). For this reason EC-EARTH3 v3.1 was not extensively tuned and documented, nevertheless it has been used in a number of EU FP7 projects (EMBRACE, SPECS, HELIX).

2.2 HadGEM3

HadGEM3 (Hadley Centre Global Environment Model version 3) is a configuration of the UK Met Office Unified Model (MetUM) which has been developed for use for both climate research and weather prediction applications. It is the result of converging the development of the Met Office's weather and climate global atmospheric model components so that, where possible, atmospheric processes are modelled or parameterised seamlessly across spatial resolutions and timescales.

The HadGEM3 family of climate models (Hewitt et al, 2011) represents the third generation of HadGEM configurations, leading on from the HadGEM2 family of climate model configurations (Martin et al., 2011) which was used for CMIP5. The HadGEM3 family comprises a range of specific model configurations incorporating different levels of complexity but with a common physical framework. It includes a coupled atmosphere-ocean configuration, with or without a vertical extension in the atmosphere to include a well-resolved stratosphere, and an Earth-System configuration which includes dynamic vegetation, ocean biology and atmospheric chemistry. A range of atmospheric resolutions is available. There is a choice of vertical resolutions between 38 levels extending to ~40km height, and 85 levels extending to ~85km in height (of which 50 are below 18km), the latter allowing improved representation of stratospheric processes. Horizontal resolutions vary between 2.5 degrees of latitude by 3.75 degrees of longitude and 0.556 degrees of latitude by 0.833 degrees of longitude, depending on the application.

The high-resolution simulations for HELIX have been performed using the HadGEM3-A Global Atmopshere (GA) 3.0 model (Walters et al., 2016) at a resolution of N216 (~60km). This is the atmospheric component of the HadGEM3 GC2 coupled climate model (Williams et al., 2015; Senior et al., 2016). Key improvements over HadGEM2 include

increased vertical levels in the atmosphere (85 compared to 38) and substantial changes to the model dynamics (ENDGame) (Wood et al., 2014). As with EC-EARTH, this version of the HadGEM3 model lies in the transition from CMIP5 to CMIP6 versions. The Met Office is operationally running the coupled HadGEM3-GC2 model at N216 resolution for seasonal and decadal forecasting and clear benefits are emerging from this use at higher resolution (MacLachlan at el., 2014; Knight et al, 2014).

3 Method

Coupled climate model simulations with high resolution are expensive yet we expect the higher resolution to better resolve land-sea contrasts, orographic variability, and small-scale processes such as convection, leading to a more realistic representation of the climate. Any coupled climate model requires a considerably long spin-up period to bring the ocean into equilibrium before any climate change simulation can start. For high resolution simulations as we would like to use them in HELIX it is still not practical to make fully coupled atmosphere-ocean integrations over long time periods due to the exorbitant costs. Furthermore, the HELIX project aims at assessing the regional climate impact and therefore needs to explore the full range of possible changes which requires making an ensemble of global high resolution simulations. To balance the need for an ensemble of high resolution simulations against the limitations of computing resources, the decision was made to make downscalings for HELIX with the high-resolution atmosphere-only versions of two climate models forced with SST and SIC from selected CMIP5 models. A similar method has been used for the CORDEX downscalings, the main difference to CORDEX is that the new simulations for HELIX are done with global high-resolution models without the need for lateral boundary forcing. Apart from the computational advantages, the use of prescribed SST and SIC at the lower boundary also constrains the high resolution downscalings to the climate of the forcing CMIP5 model which makes it easier to compare the HELIX impact results against those from other studies such as ISIMIP fasttrack.

HELIX realisation	CMIP5 forcing model	CMIP5 forcing model realisation	SWL1.5	SWL2	SWL4	SWL6
r0	ERA-Interim					
r1	IPSL-CM5A-LR	r1i1p1	2015	2030	2068	2102
r2	GFDL-ESM2M	r1i1p1	2040	2055	2113	
r3	HadGEM2-ES	r1i1p1	2027	2039	2074	2110
r4	EC-EARTH	r12i1p1	2019	2035	2083	
r5	GISS-E2-H	r1i1p1	2022	2038	2102	
r6	IPSL-CM5A-MR	r1i1p1	2020	2034	2069	
r7	HadCM3LC	(not part of CMIP5)	2003	2020	2065	
r8	MIROC-ESM-CHEM	r1i1p1	2023	2035	2071	
r9	ACCESS1-0	r1i1p1	2034	2046	2085	

Table 1: Ensemble of global high-resolution downscaling simulations (realisations) for the HELIX project with their corresponding CMIP5 forcing model. Also listed are the times when a specific SWL is passed.

Table 1 lists the selection of CMIP5 models that were used as forcing for EC-EARTH3 and/or HadGEM3 and the year of passing a specific warming level (SWL). In this work the SWL are defined as the warming relative to the pre-industrial period but alternative definitions of the SWL do exist. The details of finding the year when a SWL is passed are given in HELIX D2.1 (Gohar et al. 2014). The subset of CMIP5 models for the forcing was chosen based on different criteria such as identifying a CMIP5 model with high and another with low climate sensitivity. Other criteria were to look for an extraordinarily dry or wet climate change signal in the HELIX target regions. An important caveat is that the selection criteria were only applied in the HELIX target regions, the subset of CMIP5 models used may not be equally representative in other regions. By selecting this subset of CMIP5 models for the downscaling we sample the full range of CMIP5 models for the later forcing of impact models yet reduce the computational costs by only doing a limited number of high-resolution simulations. Tables 2 and 3 list the global and regional ranges of mean temperature and precipitation changes relative to present-day conditions in the subset of CMIP5 models that were used to force the global atmosphere-only AGCMs here. The same tables also list the results of the HELIX downscalings to illustrate the representativeness of the downscaling method and justify the use of the new HELIX ensemble in climate impact modelling studies.

The high resolution downscalings were done as transient simulations, starting in 1979 and extending to 2100 or beyond if the forcing data were available. Simulations r1-r9 all utilise the RCP8.5 scenario which represents a relatively high greenhouse gas emissions pathway for the 21st century (Riahi et al., 2011; Moss et al., 2010). The long transient simulations are a deviation from the original HELIX workplan that only foresaw the use of timeslices at each SWL. The transient simulation were not overly expensive compared to the original plan, yet they now provide the opportunity to pick other SWLs of interest that were not considered at the time when the HELIX proposal was written, e.g. the 1.5 degree warming target that was promoted in the Paris Agreement. Furthermore, the transient simulations allow us to study the time depending aspects of the climate change impact by taking into account that the different SWLs are reached at different times depending on the CMIP5 forcing model.

		CMIP5 subset		HELIX	
		min	max	min	max
Global	SWL2	1.38	2.47	1.35	2.44
	SWL4	3.94	5.24	3.93	5.11
	SWL6			6.55	6.76
Europe	SWL2	1.51	2.46	1.30	2.50
	SWL4	3.90	5.23	3.85	5.21
	SWL6			6.87	6.92
S Africa	SWL2	1.27	2.24	1.39	2.28
	SWL4	3.37	4.66	3.81	4.57
	SWL6			6.04	6.56
SE Asia	SWL2	1.10	2.01	1.07	2.05
	SWL4	3.45	3.94	3.30	4.25
	SWL6			5.72	6.21

Table 2: Range of mean temperature change at different SWLs relative to present-day conditions, global and for the three HELIX target regions. Only land-points are included the spatial averages. Listed are the range of the subset of CMIP5 models that were used as lower boundary forcing for the HELIX downscalings, and the resulting range from the two AGCMs used here

		CMIP5 subset		HELIX	
		min	max	min	max
Global	SWL2	1.62	3.77	0.77	4.43
	SWL4	2.17	8.46	4.69	8.69
	SWL6			13.75	14.46
Europe	SWL2	-2.18	5.54	-1.12	5.18
	SWL4	-7.47	8.02	-3.36	6.35
	SWL6			3.58	5.41
S Africa	SWL2	-1.45	4.28	-3.80	1.68
	SWL4	-0.83	11.54	-3.56	7.15
	SWL6			-0.81	6.75
SE Asia	SWL2	-0.56	17.40	-0.98	15.77
	SWL4	7.51	36.78	-0.25	44.09
	SWL6			10.72	23.53

Table 3: As table 2 but for the relative change of mean precipitation.

4 New high-resolution simulations compared against CMIP5

The first step in evaluating the new HELIX high-resolution simulations is to compare them with the CMIP5 models from which the SST/SIC forcings were derived. Since SST/SIC are prescribed to the atmosphere-only HELIX simulations, only changes over land areas are considered.

The two main variables of interest for climate impacts analysis are temperature and precipitation, and in order to be able to assess changes in both mean and extreme changes, these are assessed using daily data. A subset of commonly used climate extremes indices (e.g. Zhang et al., 2011) are derived from the daily variables to capture aspects of extremes based on both fixed thresholds and percentile changes. For temperature, in addition to mean annual changes (tas), the 95th percentile of daily maximum temperature is also used (tasmax95). For precipitation, mean annual precipitation (pr), the numbers of days with precipitation above 20mm (r20mm), the annual maximum 1-day precipitation (rx1day) and the 95th percentile of daily precipitation (pr95) are considered. Future work in HELIX will look at a wider suite of indices, including heat wave metrics and other user-defined threshold indices with guidance from other work packages.

The specific warming level periods for 2°C and 4°C above pre-industrial are 20-year periods which are evaluated from the original CMIP5 simulations (Gohar et al. 2014). Different simulations reach the SWLs at different times in the future (Table 1).

4.1 Temperature

For the present-day period (defined as 1981-2010), the high resolution simulations show good spatial agreement with the CMIP5 simulations in all cases (Figure 1). The benefits of higher resolution are noticeable on regional scales – for example the cooler temperatures over higher elevation regions such as the Alps and the Atlas mountains are noticeable in a number of the HELIX simulations as a result of the more detailed underlying topography in these models. The large scale patterns and magnitudes of temperatures during this base period are very similar between the CMIP5 and HELIX simulations, and are also quite consistent between the different CMIP5 models and their high resolution counterparts,

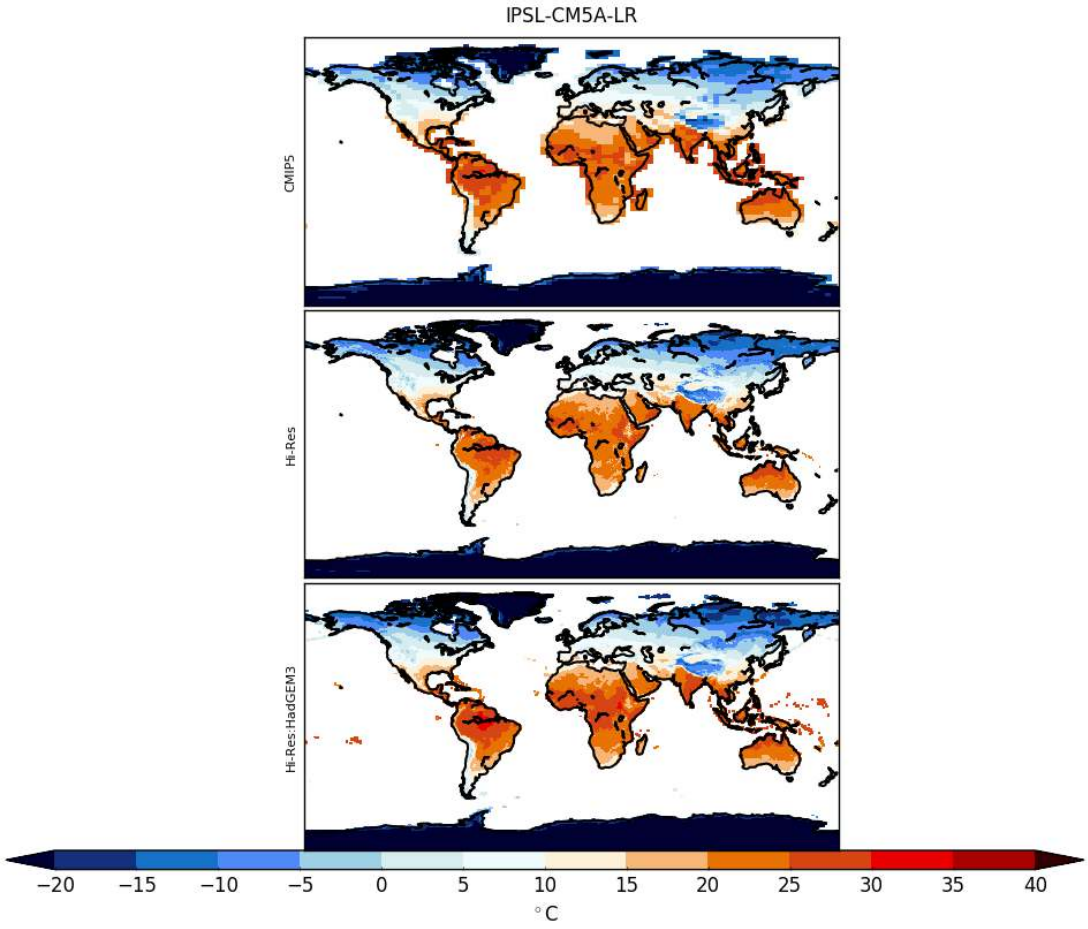

Figure 1: Mean annual temperature for the period 1981-2010 for CMIP5 IPSL-CM5A-LR simulation r1i1p1 (top), and EC-EARTH3 (middle) and HadGEM3 (bottom) HELIX high-resolution simulations driven by the CMIP5 IPSL-CM5A-LR SST and sea ice.

Global mean annual changes across the ensemble of CMIP5 models and HELIX simulations show that changes over land are generally around 2°C at SWL2 but are slightly larger than 4°C at SWL4 (Figure 2). At SWL4 land temperatures are approximately 4-6°C higher compared with present day. Magnitudes and patterns of change are broadly similar between CMIP5 and HELIX simulations (Figure 3).

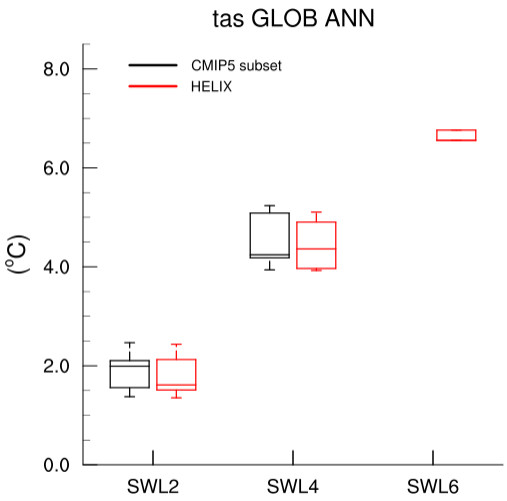

Figure 2: Mean global annual temperature change over land at SWL2, SWL4 and SWL6 relative to present-day for the ensemble of HELIX high-resolution simulations (EC-EARTH3 and HadGEM3) and the subset of CMIP5 driving models that were used in here.

The spatial maps indicate regions of 4-6°C change compared to present day at SWL4 and magnitudes and patterns of change are relatively consistent between the models. EC-Earth (CMIP5 and HELIX) tends to project slightly cooler temperature changes relative to other models at SWL2 and SWL4 (not shown). Comparing EC-EARTH3 with HadGEM3 using the IPSL-CM5A-LR driving data, the HadGEM3 simulation indicates slightly warmer temperatures compared to present day (Figure 3), and this is replicated across some of the other HadGEM3 simulations which show a slightly larger temperature response

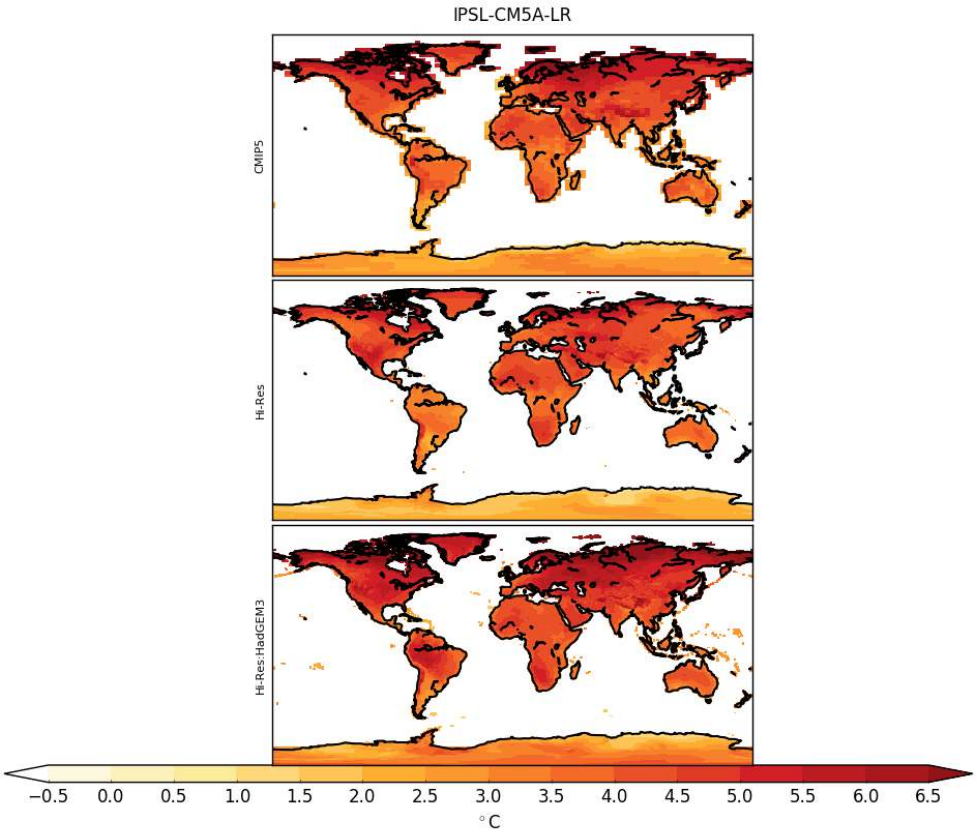

Figure 3: Mean annual temperature for SWL4 for CMIP5 IPSL-CM5A-LR simulation r1i1p1 (top), and EC-EARTH3 (middle) and HadGEM3 (bottom) HELIX high-resolution simulations driven by the CMIP5 IPSL-CM5A-LR SST and sea ice.

Temperature changes in the three HELIX sub-regions are generally in line with global changes, and similarly for seasonal summer and winter changes. South Asia (not shown) tends to show slightly smaller increases, but Europe shows generally larger increases, particularly during summer (Figure 4 top, note the high inter-model variability) where changes in some CMIP5 and HELIX simulations are above 5°C at SWL4.

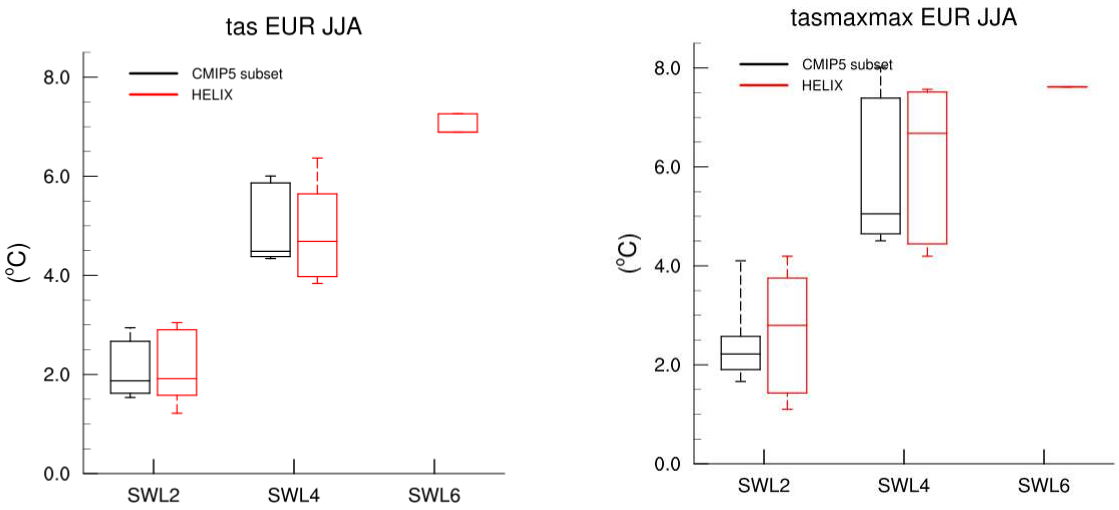

Figure 4: Mean European summer temperature (left) and maximum summer maximum temperature (right) change for the ensemble of HELIX high-resolution simulations (EC-EARTH3 and HadGEM3) and their corresponding CMIP5 driving models at SWL2, SWL4 and SWL6.

For a measure of temperature extremes, the present day global maps of the mean of daily 95th percentile temperatures again show similar patterns and magnitudes in the CMIP5 models and the HELIX simulations (not shown).

The present-day means and future changes of maximum daily Tmax for the regions and seasons are again broadly similar to global changes, with an exception being European summer temperatures (Figure 4, bottom) and annual temperatures (not shown). Again there is large inter-model variability, but at SWL2 the range of temperature change extends to around 4°C and at SWL4 the changes are much larger again with temperature changes in the range of 4.5-7.5°C.

Further work on temperature extremes will investigate changes in minimum and maximum temperatures and diurnal temperature range, plus a range of heat wave metrics.

4.2 Precipitation

Precipitation, which has a lower spatial homogeneity compared to temperature, is expected to be influenced by a move towards higher spatial resolution simulations. The spatial patterns and magnitudes of present-day annual mean precipitation compare well between the CMIP5 models and their HELIX counterparts (e.g. Figure 5). Improved representation of precipitation features associated with orgraphic ranfall in particular can be clearly seen. One particular feature across the simulations is that rainfall over India is noticeably lower in the HadGEM3 HELIX simulations compared to both the equivalent CMIP5 model and the HELIX EC-EARTH3.

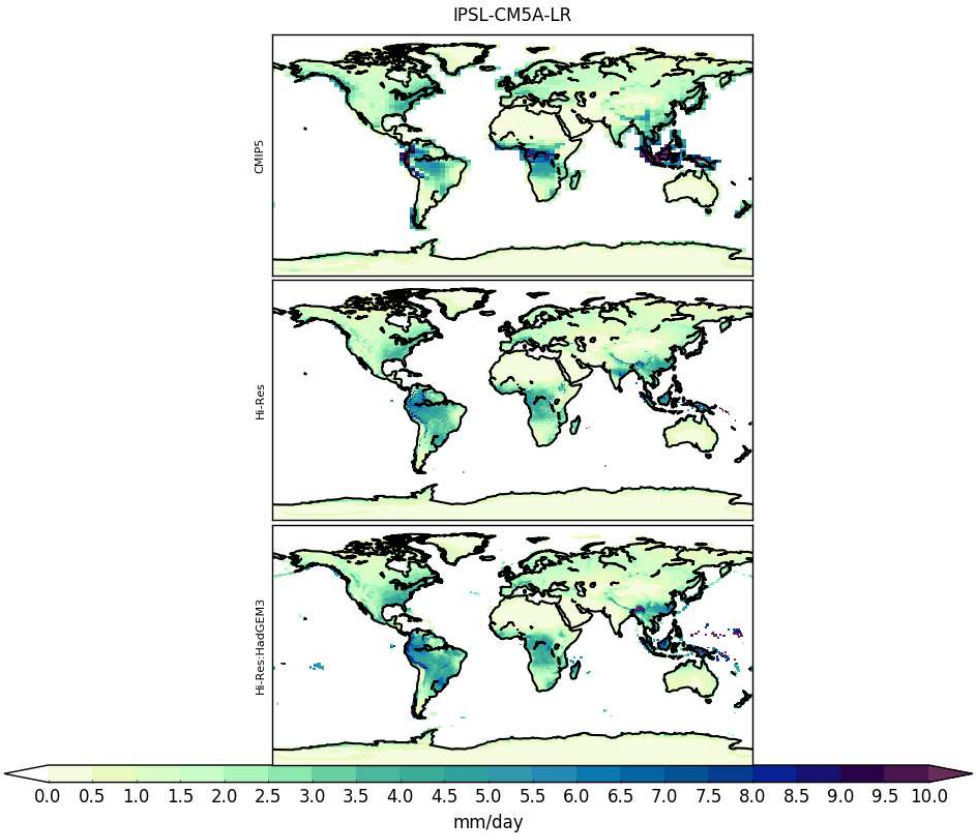

Figure 5: Mean annual precipitation for the present-day for CMIP5 IPSL-CM5A-LR simulation r1i1p1 (top), and EC-EARTH3 (middle) and HadGEM3 (bottom) Helix high-resolution simulations driven by the CMIP5 IPSL-CM5A-LR SST and sea ice.

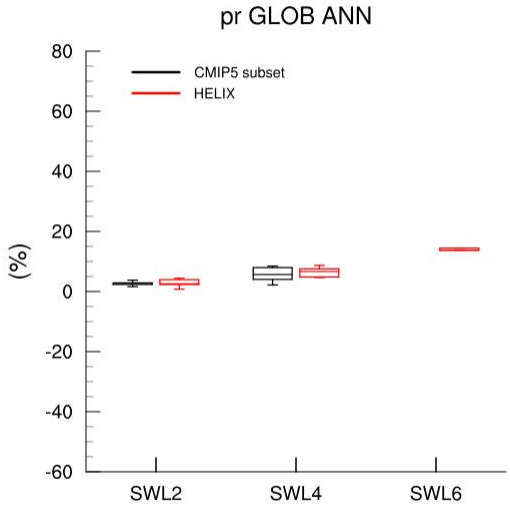

Figure 6: Mean relative global annual precipitation change over land at SWL2, SWL4 and SWL6 for the ensemble of HELIX high-resolution simulations (EC-EARTH3 and HadGEM3), their corresponding CMIP5 driving models, and the full range of CMIP5 models.

Changes in precipitation globally (expressed as a percentage) are quite small at SWL2, with increases in the 0-5% range, and slightly larger at SWL4 (Figure 6). Changes of 10-20% are seen in the limited sample of HELIX models which reach SWL6. However, the regional patterns vary considerably, with projected changes for Europe showing increases in winter rainfall, and decreases in summer (Figure 7). The largest changes for Europe can be seen in summer rainfall reductions to as much as 20% or more at SWL4.

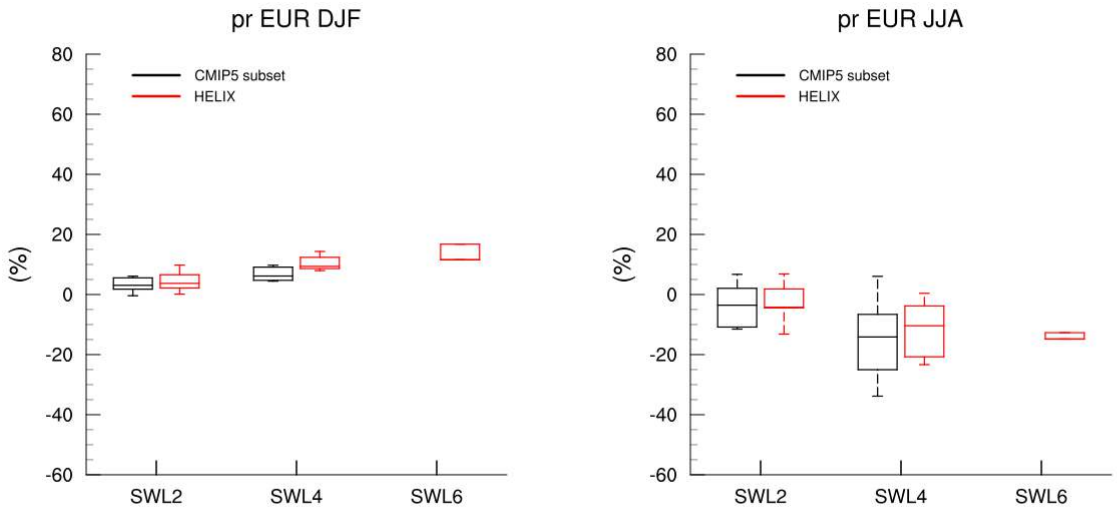

Figure 7: Mean European winter (left) and summer (right) precipitation changes at SWL2, SWL4 and SWL6 for the ensemble of HELIX high-resolution simulations (EC-EARTH3 and HadGEM3), their corresponding CMIP5 driving models.

For sub-Saharan Africa (not shown), large percentage increase are projected in winter rainfall (as high as 70-80% at SWL6), but these are relative to low winter rainfall totals. Annual and summer changes project modest increases at SWL4 and SWL6. South Asia shows projected decreases in winter rainfall, but quite large increases in summer rainfall (Figure 8). There is a large range in the HELIX model projections. One reason for this may be the relatively dry conditions over South Asia simulated by the HadGEM3 model compared to EC-EARTH

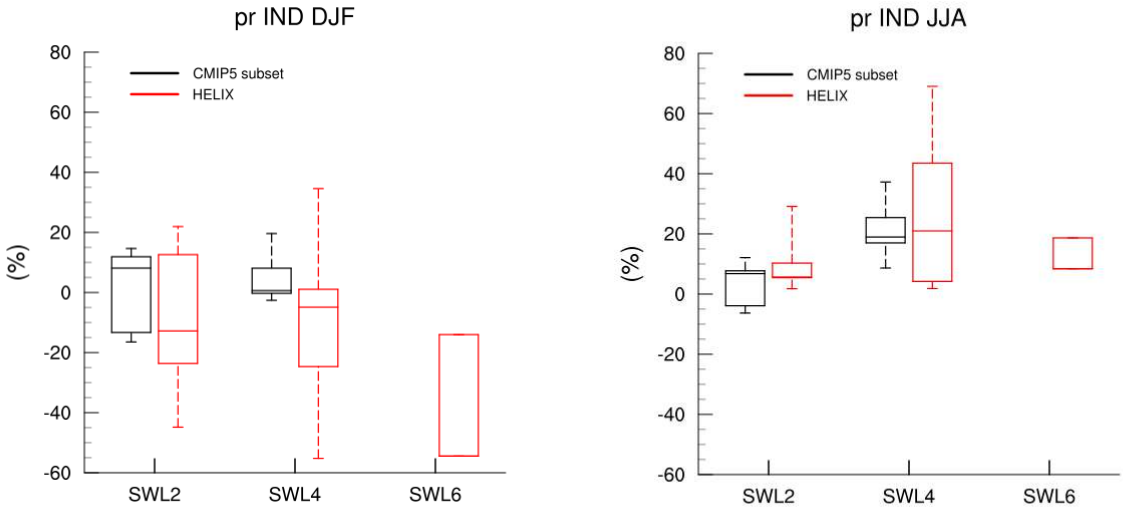

Figure 8: Mean South-East Asia winter (left) and summer (right) precipitation changes at SWL2, SWL4 and SWL6 for the ensemble of HELIX high-resolution simulations (EC-EARTH3 and HadGEM3), their corresponding CMIP5 driving models.

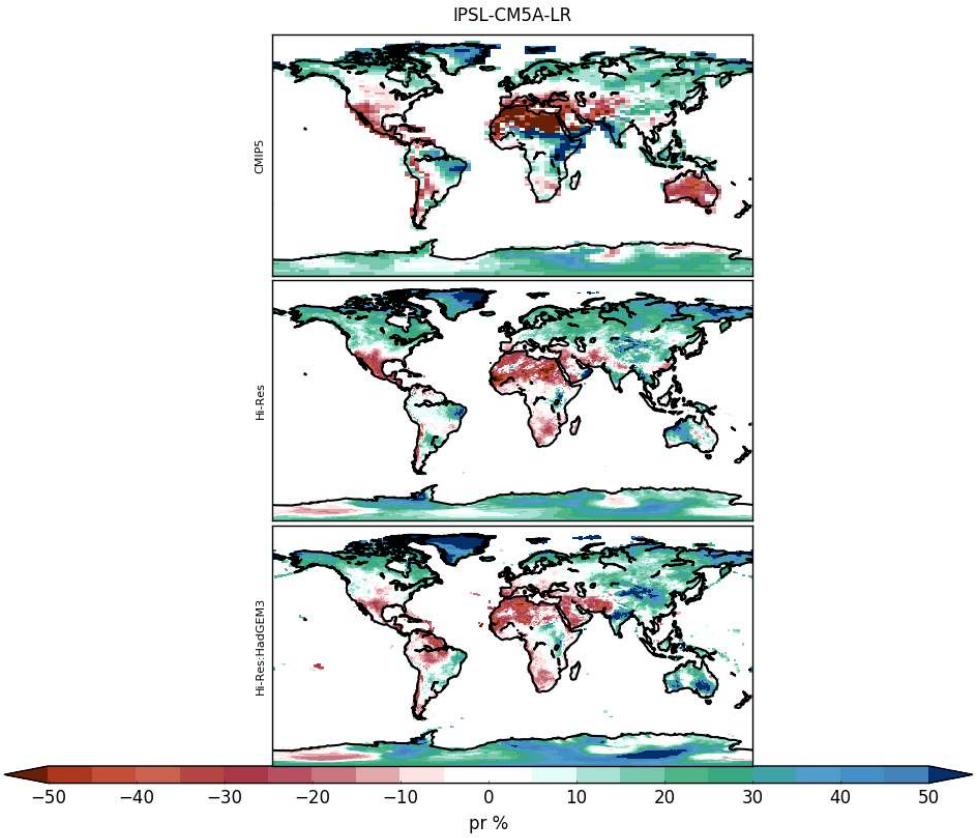

Figure 9: Mean annual precipitation changes for SWL4 for CMIP5 IPSL-CM5A-LR simulation r1i1p1 (top), and EC-EARTH3 (middle) and HadGEM3 (bottom) HELIX high-resolution simulations driven by the CMIP5 IPSL-CM5A-LR SST and sea ice.

There are some large regional differences in precipitation changes (Figure 9). Australia is a notable exception, being drier in the IPSL-CM5A-LR CMIP5 simulation at SWL4, but wetter in the two HELIX simulations. There are also quite large differences over sub-Saharan and east Africa.

The r20mm index (number of days per year with over 20mm of rainfall) shows large scale agreement in spatial patterns and magnitudes for the present day simulation period. A comparison of the MIROC-ESM-CHEM model in CMIP5 and HadGEM3 (Figure 10) shows clearly the much better spatial definition of features. The hi-res simulation shows a higher number of heavy rain days in southern Europe and higher frequency of heavy rain over south America. Again notice the lack of heavy rainfall days over South-East Asia in the HadGEM3 simulation.

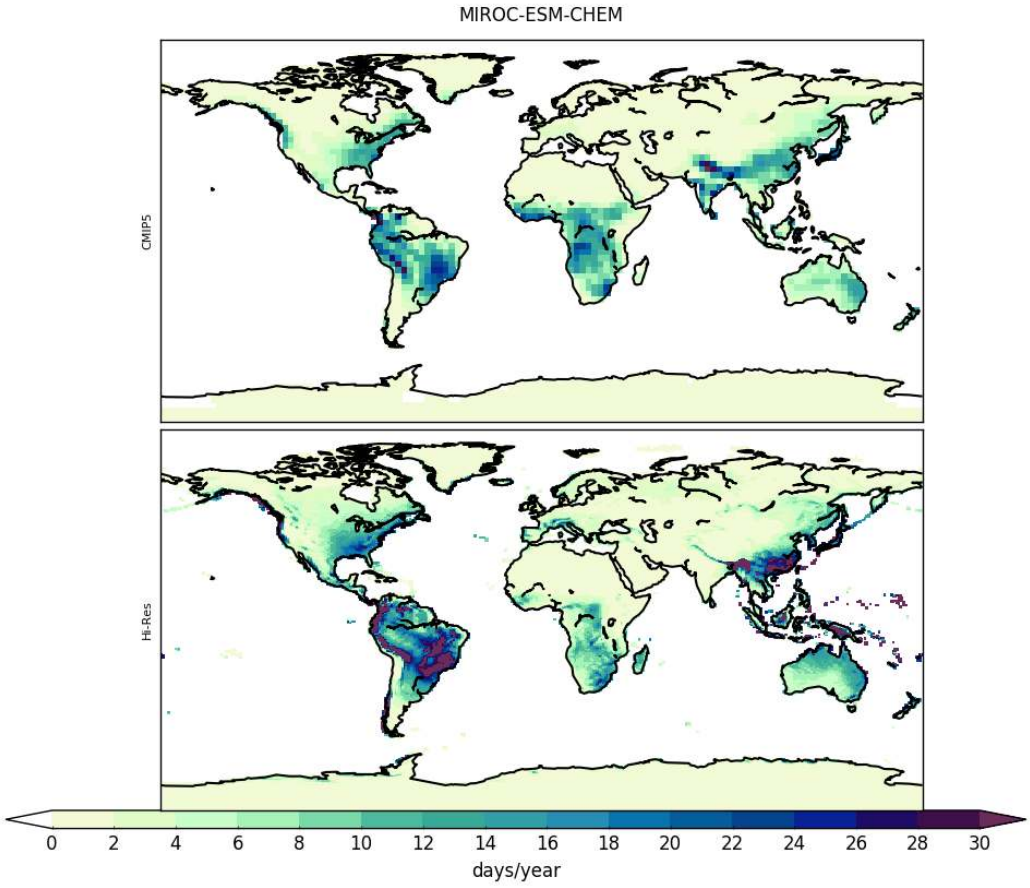

Figure 10: Mean annual R20mm changes (days per year) for the present-day for CMIP5 MIROC-ESM-CHEM simulation r1i1p1 (top), and corresponding HadGEM3 (bottom) HELIX high-resolution simulation.

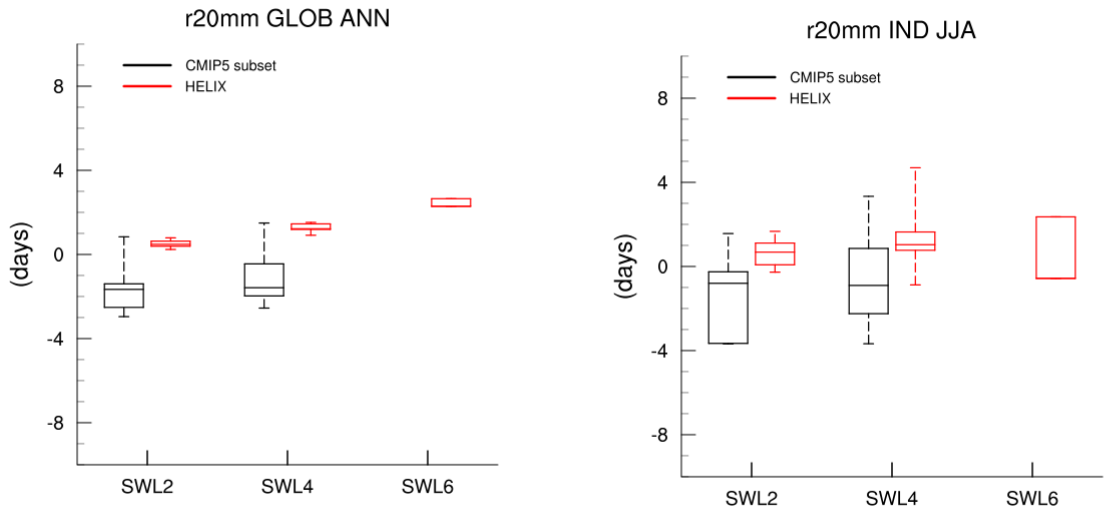

Figure 11: Mean global annual (left) and South-East Asia summer (right) change in the number of days with 20mm or more precipitation (r20mm) changes for the ensemble of HELIX high-resolution simulations (EC-EARTH3 and HadGEM3) and their corresponding CMIP5 driving models at SWL2, SWL4 and SWL6.

A feature of the high resolution simulations is a generally larger increase (or less of a decrease) in the frequency of heavy rain days in the future compared to the CMIP5 projections (Figure 11, top). This is the case across all of the sub-regions as well. South Asia also shows a pattern of increasing heavy rain days at the SWLs in the HELIX simulations, but decreases in the CMIP5 models (Figure 11, bottom).

The 95th percentile of precipitation shows similar good agreement to mean annual precipitation for the present day. HadGEM3 shows wetter conditions over a number of regions, but again is relatively dry over South Asia (Figure 12).

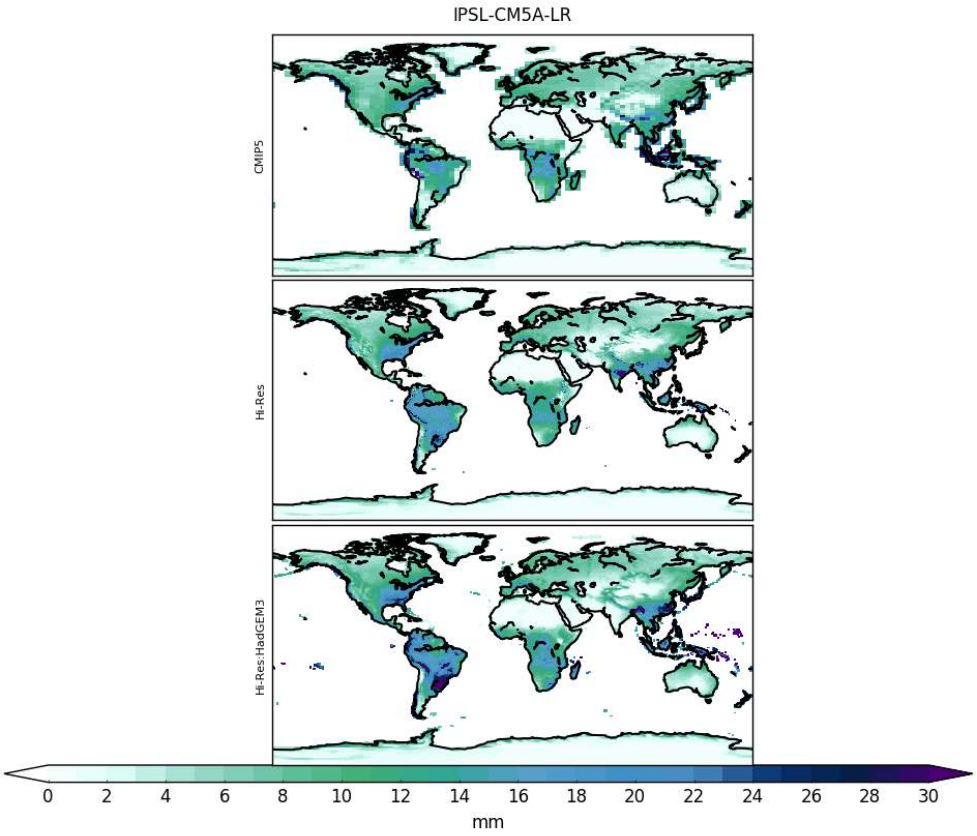

Figure 12: Mean annual 95th percentile of precipitation for the present-day for CMIP5 IPSL-CM5A-LR simulation r1i1p1 (top), and corresponding EC-EARTH3 (middle) and HadGEM3 (bottom) HELIX high-resolution simulation.

The changes at the SWLs show interesting regional variations for rx1day (maximum one day rainfall). For sub-Saharan Africa, there are modest decreases in this index at SWL2 and increases at the higher SWLs (Figure 13, top).

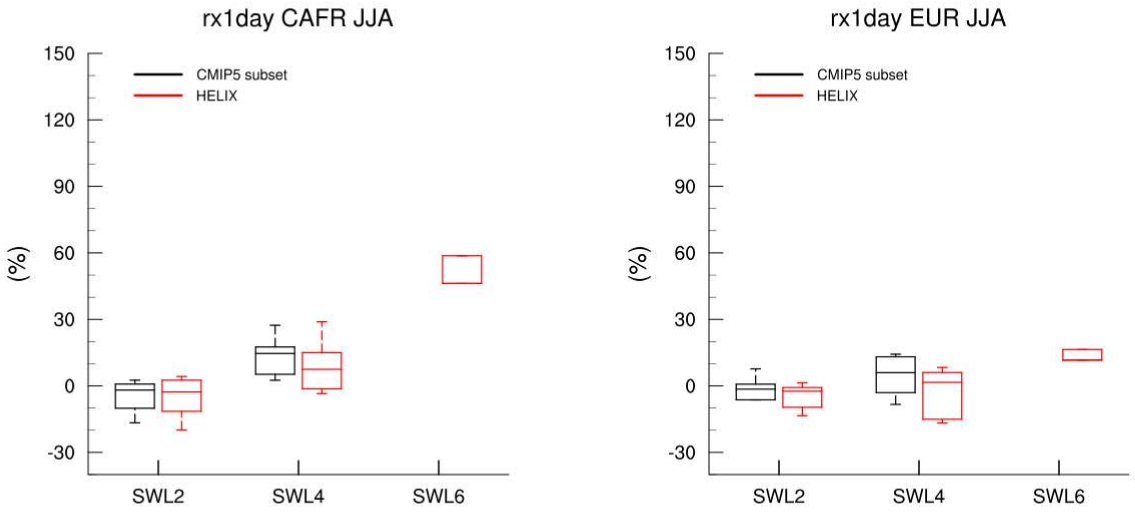

Figure 13: Mean northern sub-Saharan African(left) and European (right) changes of summer maximum day precipitation(rx1day) for the ensemble of HELIX high-resolution simulations (EC-EARTH3 and HadGEM3) and their corresponding CMIP5 driving models at SWL2, SWL4 and SWL6.

Europe also shows a slight decrease at SWL2, and then an ambiguous change at SWL4 for changes in summer rainfall (Figure 13, bottom). Winter (not shown) shows increases towards higher SWLs. South Asia points towards increases in rx1day during summer (Figure 14, top). During the winter, and based on smaller rainfall totals, the pattern is less clear, with a difference in the sign of change between CMIP5 and HELIX simulations at SWL4 (Figure 14, bottom).

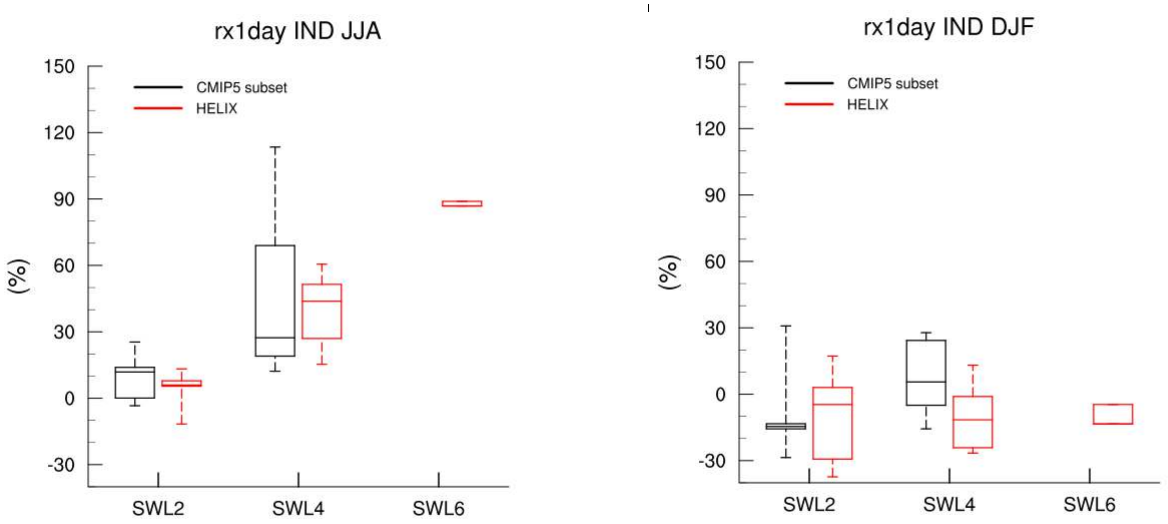

Figure 14: Mean South-East Asia summer (left) and winter (right) rx1day changes for the ensemble of HELIX high-resolution simulations (EC-EARTH3 and HadGEM3) and their corresponding CMIP5 driving models at SWL2, SWL4 and SWL6.

5 Sensitivity to model resolution in the EC-EARTH3 model

The two climate models used for the high-resolution downscaling in HELIX are developments of CMIP5 models and belong to the next generation models that will be used for CMIP6. The parameterisations and the description of processes have been improved and thus it is not straightforward to attribute all changes between downscaled HELIX simulations and the original CMIP5 models only to the increased resolution. To separate the impact from higher resolution from other improvements of the climate models we study the differences between two downscaling that were both done with the same EC-EARTH3 model yet different horizontal resolution, T255 (≈ 80 km at the equator) and T511 (≈ 40 km at the equator). The SST and sea-ice forcing for these simulations are from the EC-Earth, GFDL-ESM2M and IPSL-CM5A-LR models from the CMIP5 archive.

The two ensembles (with three simulations each) are analysed to study the gain from higher resolution; both when looking at the general features (such as mean values) over large regions and also in the probability distribution of variables. The focus is on the 3 HELIX target regions Europe, Southern Africa and South-East Asia. Model results for

the present-day climate are compared with ERA-Interim reanalysis at 80 km resolution (Dee et al. 2011), and for Europe also the EOBS reanalysis at 25 km horizontal resolution (Haylock et al. 2008).

A natural consequence of higher resolution is that the topography is better resolved; especially the extent and altitude of mountain ranges are better described with higher resolution. EOBS, having the highest resolution of all datasets considered here has the most realistic description of topography. As an example if we compare the topography in the T255 and T511 resolutions we conclude that the Pyrenees are around 1000 m higher with T511 and that the Carpathians has a shape more similar to reality. In southern Africa the coastal mountain ranges get higher and steeper. In India the largest differences are found around the mountain ranges on the west coast and in the north east.

It is not possible to directly compare the same variable with two different resolutions unless the fields are remapped onto a common grid with all the negative consequences that follow with the interpolation. Thus, the comparison between the simulations of different resolutions is made in two ways: partly by qualitatively comparing maps, and in a more quantitatively way comparing probability density functions (PDFs) of the different simulations. For each grid point in one of the domains a set of metrics are computed, e.g. mean temperature, maximum precipitation, number of precipitation days etc. The PDFs express the ability of the simulations to capture the frequency of occurrence of a given metric. In that way simulations with different resolution and different number of gridpoints can be compared, with the caveat that two simulations can have the same PDF but completely different spatial distributions. The PDFs should therefore be complemented by maps to at least qualitatively see if the spatial patterns are similar.

For this section the present-day climate is defined as the climate of the period 1981-2010. The specific warming levels (SWL) are defined as the 20-year period around the date when the running mean of the global mean temperature of the forcing CMIP5 model reaches a specific warming compared its pre-industrial climate (Gohar et al. 2014). This means that the timing of the SWLs can differ between simulations that are forced with SST and SIC from different CMIP5 models. The SWLs used here are 2, 4 and 6 °C warmer than pre-industrial.

5.1 Impact of the resolution in present-day climate

5.1.1 Temperature

Europe

The general features of annual temperature in Europe are similar in all simulations and reanalyses: warmer in the south and colder in the north; the Alps and Carpathians colder than the surrounding areas and sea areas warmer than land areas (Fig. 15). Generally the model simulations are colder than the reanalyses. There are also differences between the model simulations caused by differences in the SST/SIC from the forcing CMIP5 model. The large scale atmospheric circulation, which determines a large part of the simulated climate, is the same regardless of the resolution. Within the same model set-ups there are differences between resolutions, but these are attributed to differences in topography; the temperature follows the topography field which doesnot change the main features of the temperature field. The inter-model differences at one resolution are larger than the differences between resolutions.

Figure 16 (left) shows that the driving model is of most importance for the simulated climate; the two simulations for each model set-up are paired together. The simulated temperatures are generally too cold and the simulations largely underestimate the occurrence of temperatures above 15 °C and overestimate temperatures below 0 °C. There are differences between the reanalysis data sets that are mainly due to differences in resolution.

For summer maximum temperature (here defined as the 95th percentile of maximum temperature), the model simulations underestimate the temperature of the most common temperature (Fig. 18, right). In the “cold” side of

the distribution all models compare well with ERA-Interim, but have a too high probability of temperatures in the range 10-25 °C compared to EOBS. The models peak at a lower temperature than the reanalyses which means that the models largely underestimate the occurrence of temperatures in the range 25-30 °C. There are differences between the reanalyses also on the "warm" side of the distribution, here the models compare well with EOBS. The differences in summer maximum temperature between models and resolutions are small.

Since the temperature does not change much with higher resolution, indices based on temperature will not change much either. We found no significant changes in e.g. the length of the growing season and heat wave duration index.

Southern Africa

The same conclusions about the general temperature pattern as for Europe can be made for Africa. The models capture the spatial distribution of annual mean temperature yet are too cold in most of the domain. The simulations overestimate the probability of temperatures below 20 °C and underestimate the probability of temperatures above 25 °C. There are clear differences between the model set-ups; most notably the EC-EARTH driven simulations are colder than the others. The difference between resolutions is small however; the differences between CMIP5 forcing models are larger than the differences between the two resolutions.

South-East Asia

The models capture the general features of annual mean temperature, but are too cold in most of the domain. The models overestimate the probability of temperatures below 25 °C and underestimate the probability of temperatures above 25 °C. Neither ERA-Interim interim nor the simulations shows temperatures above 30 °C. The EC-Earth forced simulations are colder than those forced with other CMIP5 models. On the other hand the difference between the spatial resolutions is smaller.

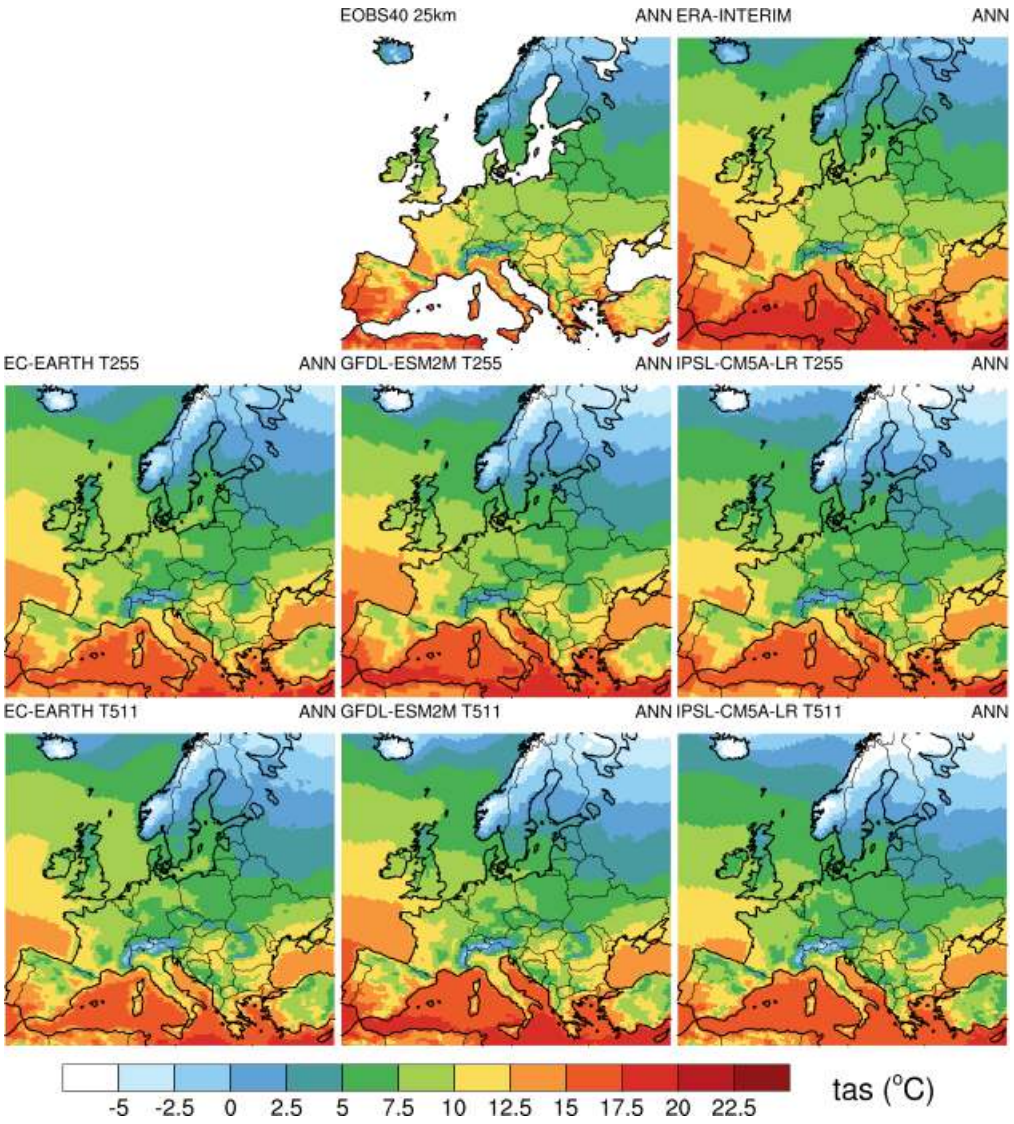

Figure 15: Annual mean temperature (°C, tas) in Europe for EOBS (top centre), ERA-Interim (top right), low resolution (T255) simulations (middle) and high resolution (T511) bottom. The CMIP5 models for the SST/SIC forcing of the simulations shown in the two bottom rows are EC-EARTH (left), GFDL-ESM2M (middle) and IPSL-CM5A-LR (right).

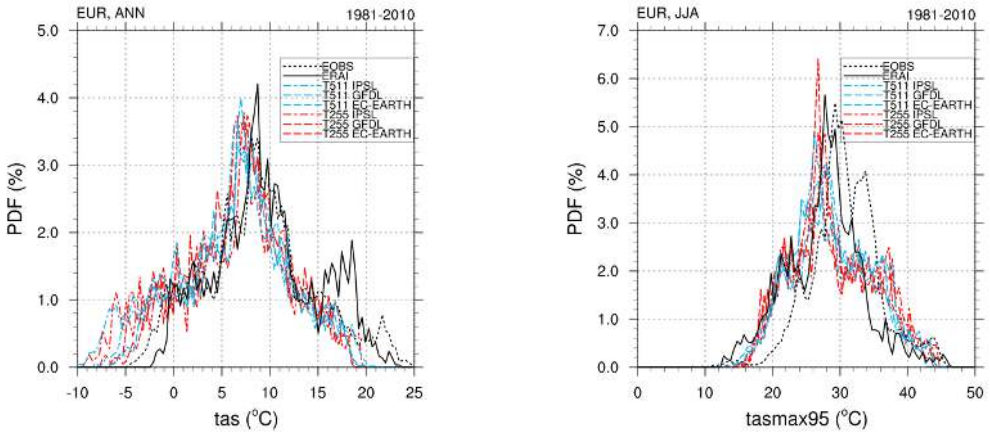

Figure 16: PDF of annual mean temperature (tas, left) and the 95th percentile of maximum summer temperature (tasmax95, right) over Europe for EOBS (black dotted line), ERA-Interim (black full line), high resolution simulations (T511, blue lines) and low resolution simulations (T255, red lines). The CMIP5 model for the forcing of the different simulations is listed in the legend.

5.1.2 Precipitation

Europe

The models are able to reproduce the spatial pattern of precipitation given by the reanalysis data sets. Precipitation amounts range from 0.5 to 5 mm/day. The largest precipitation amounts are found in mountainous areas and on the west coasts of Scandinavia, the British Isles and the Iberian Peninsula. The smallest precipitation amounts are found in Northern Africa and Southeast Europe.

For obvious reasons higher resolution is expected to improve the spatial distribution of precipitation (Fig. 19). The precipitation pattern is more detailed and more realistic with higher resolution, especially at coast lines and in mountainous areas. In low resolution simulations precipitation is smoothed out over large areas, while in higher resolution precipitation follows the more complex topography, which means that precipitation gets more localised in space and that the precipitation amounts increases in some areas. This effect is visible also in the reanalysis data sets. As an example the amount of precipitation on the east side of the Adriatic Sea is in some regions twice as much in the high resolution simulations compared to the low resolution simulations.

When looking at the 95th percentile of the annual precipitation (a measure of extreme precipitation) it is seen that there is a general agreement between models and reanalysis, the distributions have similar widths, they all peak at about the same point and have roughly the same maximum (Fig 20). At a closer look the models tend to give too little precipitation for the most common precipitation amounts. The largest differences are found in the “wet” tail of the distribution; here the high resolution simulations give higher values for the most extreme precipitation which is more similar to the EOBS reanalysis. The highest value of the 95th percentile is around 22 mm in ERA-Interim and the low resolution simulations and at least 32 mm in EOBS and the high resolution simulations. It is interesting to note that this effect also appears in the reanalysis data sets, the more resolved EOBS reanalysis gives higher precipitation than the less resolved ERA-Interim reanalysis which suggests that this really is an effect of the higher resolution.

The number of days with precipitation more than 10 mm (r10mm) is fairly similar between models and reanalysis; the largest differences are not found at the high-end tail of the distribution, but rather on the most frequent number of days. That part of the distribution also has the largest differences between models. The EC-EARTH and IPSL driven simulations peaks at around 9 days and the GFDL driven simulations peak at around twelve days, while ERA-Interim peak at 10-12 days.

For the numbers of days with precipitation more than 20 mm (r20mm) the low resolution simulations hardly give any occurrences of more than 20 days per year days with precipitation above 20 mm while the high resolution models give more than 30 days, which is more in line with the EOBS reanalysis. A similar pattern is found for the maximum 5 day precipitation (rx5day). Low resolution simulations give a maximum of at most 220 mm and the high resolution simulations up to 320 mm and EOBS as much as 400 mm.

Southern Africa

In Africa the temperature differences between model simulations and reanalyses are bigger. In particular the models underestimate the precipitation amounts in the north western part of the Southern Africa domain. In some parts the simulated precipitation is only half of the amount of the reanalyses. The models do not capture the full spatial variability; they underestimate the occurrence of precipitation events with more than 5 mm/day and less than 1 mm/day. On the other hand there is an overestimation in the models in the probability for precipitation with 3-7 mm/day. This is connected to the simulated precipitation in the north western part of the domain; instead of simulating precipitation amounts in the range 5-10 mm/day the simulate precipitation in the range 3-5 mm/day. The models have also problems with simulating the small precipitation amounts in the south western parts of Africa. Although the high resolution simulations give a more detailed spatial distribution they do not perform better.

Similar problems are seen in the distribution of precipitation days. The models underestimate the occurrence of very dry (< 20 precipitation days per year) and very wet (more than 300 precipitation days per year) regions. There is some improvement in the high resolution simulations, which have higher frequency of precipitation days over 280 days per year compared to the low resolution simulations. From the maps showing the spatial distribution of precipitation days we see that the models underestimate the number of wet days in the north western part of the domain and the number of dry days in the south western part compared to ERA-Interim. This is for the same reasons as the differences in precipitation amounts; with less precipitation comes fewer precipitation days (in the north east) and more precipitation gives more precipitation days (in south west).

For the number of days with precipitation over 20 mm there are considerable differences between the high and low resolution simulations. The low resolution simulations have a higher probability of having more days with precipitation over 20 mm. The high resolution simulations give fewer days which is more in line with ERA interim.

It appears that although the annual precipitation is similar in the high and low resolution simulations there are differences in how the precipitation is distributed in space and time. This also shows in the 95th percentile of daily precipitation, where the high resolution simulations have distributions more similar to ERA interim.

South-East Asia

In South-East Asia there is a general agreement between model simulations and reanalyses on the distribution and amount of precipitation. The simulations do not capture the dry region in the northwest found in ERA-Interim with precipitation close to zero. The simulations give more precipitation, especially on the west coast. This orographic precipitation is enhanced in the high resolution simulations. There is a clear difference between the resolutions in how they simulate the largest precipitation amounts. The high resolution simulations give precipitation up to 11 mm/day while the low resolution simulations and ERA-Interim give up to 8 mm/day.

For the number of days with precipitation over 10 mm there are differences between the high and low resolution simulations. Only the high resolution simulations capture the regions with more than 100 days of precipitation over 10 mm, which is also seen in ERA-Interim. A similar pattern is seen in the maximum five day precipitation. Only the high resolution simulations capture the highest precipitation amounts and the high resolution simulations also match ERA-Interim better than the low resolution simulations.

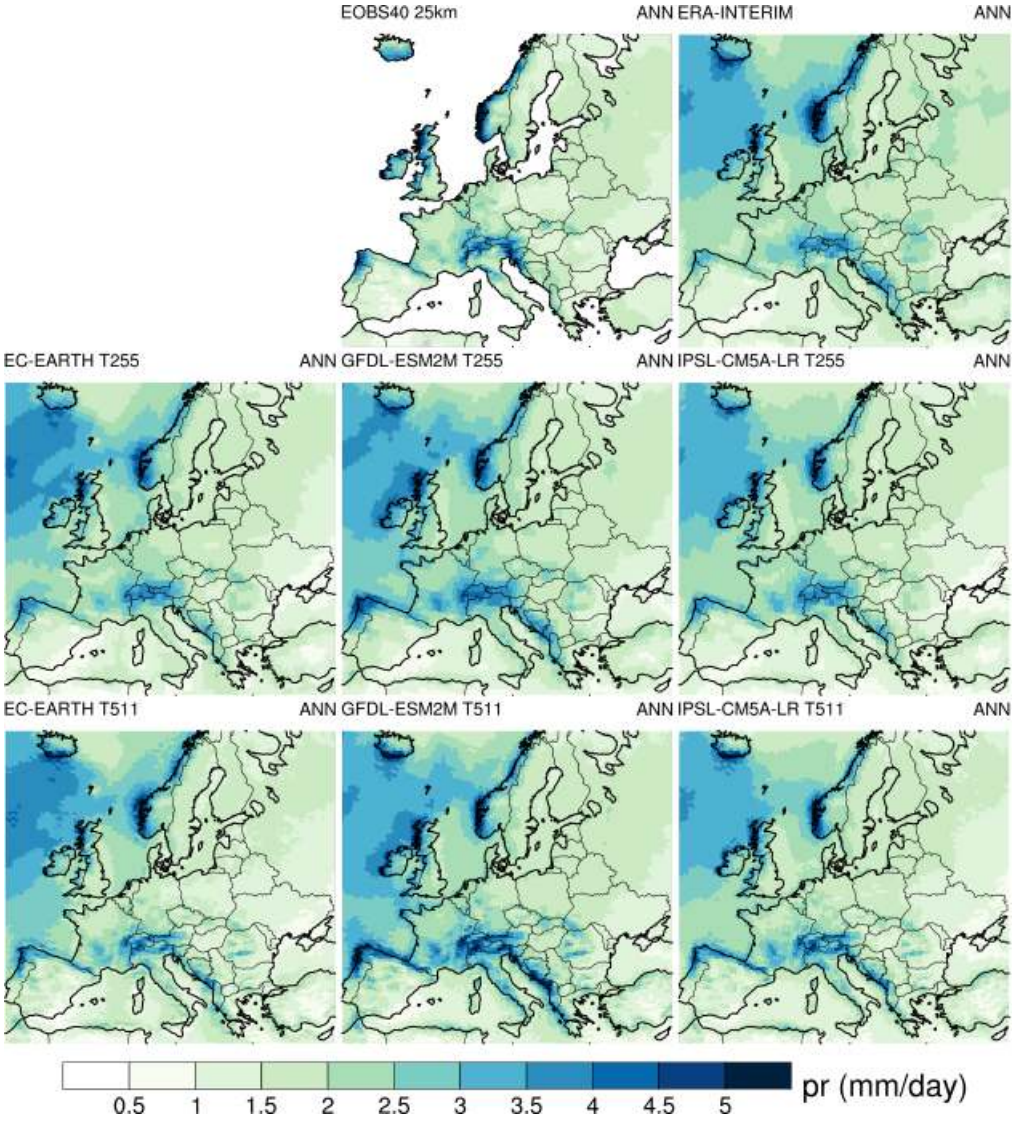

F*igure 17: Annual precipitation (mm/day, pr) in Europe for EOBS40 (top centre), ERA-Interim (top right), low resolution (T255) simulations (middle) and high resolution (T511) bottom. The driving models in the two bottom rows are: EC-EARTH (left), GFDL-ESM2M (middle) and IPSL-CM5A-LR (right).*

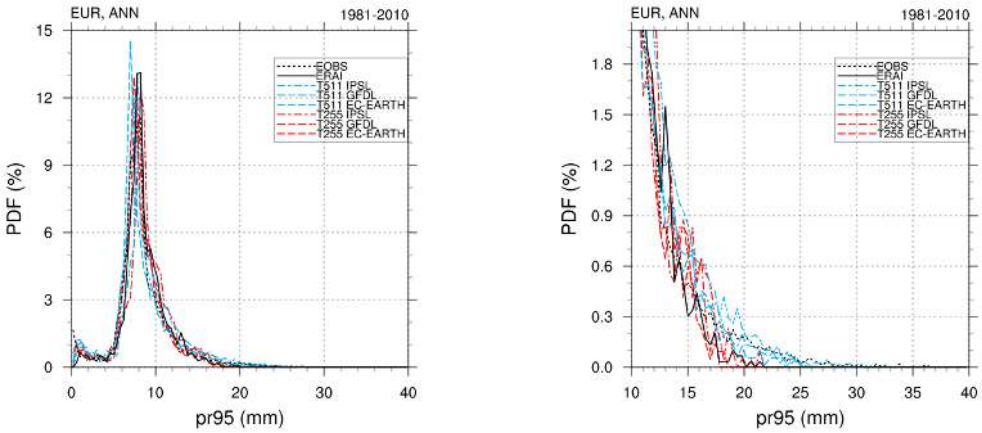

Figure 18: Left: PDF of the 95th percentile of annual precipitation (mm/day, pr95) in Europe for EOBS (black dotted line), ERA-Interim (black full line), high resolution simulations (T511, blue lines) and low resolution simulations (T255, red lines). Right: same as left, but zoomed in on the end of the tail.

5.2 Impact of the resolution in projections of the future

To test if the climate change signal depends on model resolution we investigate the difference between high and low resolution simulations at SWL2, SWL4, and SWL6. Of the three model configurations used here two reach SWL4 and only one reaches SWL6. This makes the comparison less robust since there is only one model set-up with all three SWLs.

5.2.1 Temperature

Europe

Europe will be warmer in the future. At SWL2 the annual temperature will be 1-3 °C warmer than the period 1981-2010 with the RCP8.5 scenario. The amplitude of the warming differs between simulations with different SST/SIC forcings, but not so much between different resolutions and the same forcing. Particularly the GFDL driven simulations show a stronger warming than the two other model set-ups. There are common features in all simulations, such as strongest warming in the northern parts of the domain (Arctic amplification) and a strong warming over the Iberian Peninsula. Notable differences are the GFDL-driven simulations that show a strong warming over Eastern Europe while in the IPSL-driven simulations this is the region with little warming. The PDFs are shifted about 2 °C to the right (warmer) for every SWL (Fig 19, top). The shapes of the SWLs are more or less retained, but this is a bit difficult to evaluate since the number of models are reduced in the higher SWLs. It is clear, however, that the effect of resolution is small. For one model set-up the difference between simulations with different resolutions is small, while there are clear differences between simulations with different model set-ups.

Southern Africa

Temperature is projected to increase in all parts of the Southern African domain in the future. At SWL2 the annual temperature will be 1-3 °C warmer than the period 1981-2010 according to scenario RCP8.5. The models generally agree on the pattern of temperature change, which includes stronger warming in the southwest and northwest. The temperature response is larger in the GFDL-driven simulations and slightly less in the other two set-ups. The differences between the model set-ups are larger than the differences between resolutions within the model set-

ups. The PDFs are shifted about 2 °C to the right (warmer) for every SWL (Fig. 19, middle). The shapes of the PDFs are more or less retained.

South-East Asia

The temperature over South-East Asia is expected to increase in the future. At SWL2 the annual temperature will be 0.5-2.5 °C warmer than the period 1981-2010. The simulations generally agree on the pattern of temperature change, which includes stronger warming over land than over ocean. The temperature response is largest in the GFDL-driven simulations and slightly less with the other two forcing models. Again we find that the differences between simulations with different SST/SIC forcing is larger than the differences between resolutions.

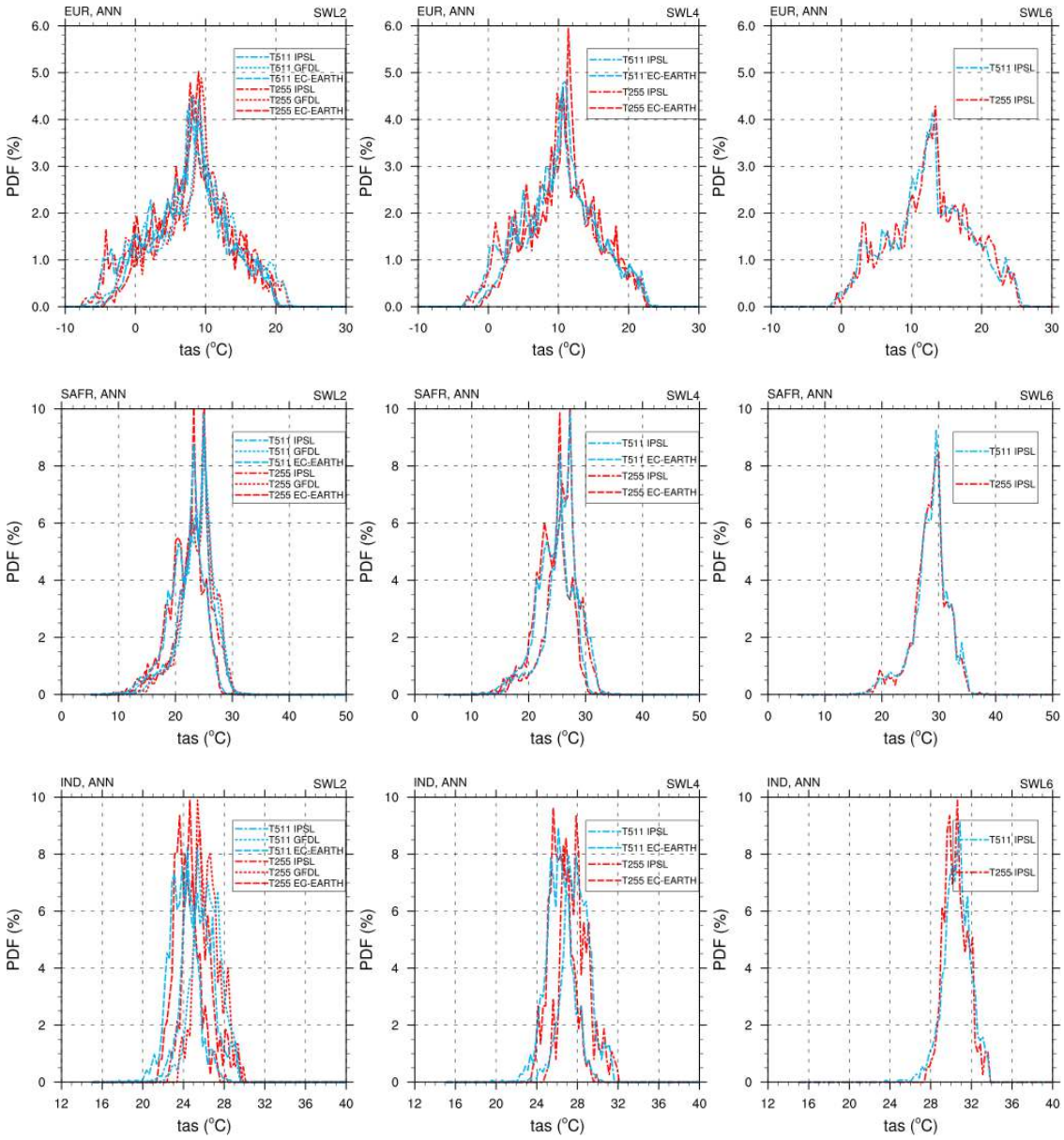

Figure 19: PDF of the annual mean temperature (°C, tas) over Europe (top), Southern Africa (middle) and South-East Asia (bottom) for high resolution (T511, blue lines) and low resolution simulations (T255, red lines) for SWL2 (left), SWL4 (middle) and SWL6 (right). The legend denotes the forcing CMIP5 model.

5.2.2 Precipitation

Europe

The precipitation change is not as uniform as the temperature change. Generally annual precipitation is expected to increase (+10-30%) in the North and East and decrease (-10%) in the West and South. This pattern is even more pronounced in the higher SWLs. The different model set-ups give somewhat different estimates of this. For example: the GFDL–forced simulations give increasing precipitation over the Iberian peninsula while the other model set-ups give decreasing precipitation, and the EC-EARTH-driven simulations give increasing precipitation east of Iceland while the GFDL-driven simulations give increasing precipitation. There are similarities between resolutions within the model set-ups, but the higher resolution simulations tend to give larger changes in both directions. This dual change pattern means that the shapes of the PDFs will change with higher SWLs. The probability for the highest precipitation will not change much, but the most probable precipitation amounts will be shifted to the wetter end at the same time as the probability for low precipitation increases. Still, the effect of resolution is low.

The number of days with precipitation over 10 mm changes in the same way as the mean precipitation: more where precipitation increases and less where precipitation decreases. With higher SWLs this pattern is even stronger, in areas with decreasing (increasing) number of days the number of days decrease (increase) even further. This means that the PDF gets wider with higher SWLs since both less days and more days of 10 mm precipitation will get more common. The effect of the resolution is small at SWL6. The same pattern of change as for precipitation amount and precipitation days above 10 mm is seen for the 95th percentile of annual precipitation and the number of days with precipitation over 20 mm.

The maximum five day precipitation changes in a more random way, but the tendency is that the maximum five day precipitation is likely to increase with higher SWLs across the domain (Fig 20). With higher SWLs the regions of decreasing five day precipitation gets smaller and fewer. This means that the maximum five day precipitation will increase even in regions where precipitation will decrease. The difference between resolutions is investigated more closely for the PDFs of the maximum five day precipitation. For this index there is a clear difference between low and high resolution simulations already in the control period. At SWL2 all curves are shifted to the right indicating that extreme precipitation will increase in Europe in a warmer world. All curves are shifted by a similar amount which means that the climate signal is the same independent of resolution. Note that the difference between low and high resolution simulations remains also in the future; even if the climate change signal is the same the high resolution simulations will still give higher probability of extreme precipitation.

Southern Africa

At SWL2 there are considerable differences in the pattern of precipitation change between the model set-ups. The EC-EARTH-driven simulations give decreasing precipitation of around 10% in most of the domain while the GFDL-driven simulations give increasing precipitation with up to 40% in the north eastern part, while the IPSL-driven simulations are somewhere in between. There are also significant differences between resolutions. In the IPSL-driven simulations the low resolutions simulation gives decreasing precipitation in the south while the high resolution simulation gives increasing precipitation. These differences are, however, probably an effect of the weak climate change signal at SWL2, the differences between model set-ups and resolutions are reduced at higher SWLs. At SWL4 the EC-Earth-driven simulations are much more similar to the IPSL-driven simulations at both resolutions. The conclusion of this is that the long term change in precipitation is projected to be decreased precipitation in the southwest and northeast, with a region of increasing precipitation between.

The number of precipitation days (precipitation more than 1 mm/day) are projected to decrease in the future: this is not so easy to see from the PDFs, but it is clear from the maps. The number of precipitation days is projected to

decrease in most of the domain. At SWL4 the number of precipitation days increases more or less everywhere except for the region around Lake Victoria. The number of precipitation days will decrease even in regions with increasing precipitation, which implies that the precipitation dynamics will change so that more precipitation will fall at fewer occasions. The differences between different resolutions are small.

The number of days with precipitation over 10 mm changes in the same way as the mean precipitation: more where precipitation increases and less where precipitation decreases; the same goes for the 95th percentile of annual precipitation and the number of days with precipitation over 20 mm. For the 95th percentile of annual precipitation and days with precipitation over 20 mm there are clear differences between the high and low resolution simulations in the control period. These differences remain in the future climate, but decreases with higher SWLs. One reason for this could be that the area of increasing precipitation is getting larger which means that a high model resolution is less important for detecting it.

The maximum five day precipitation changes in a more random way, at SWL2 there is as much increase as decrease (Fig. 20). It is clear, however, that the maximum five day precipitation will increase with higher SWLs. At SWL6 the IPSL-driven simulations show increasing five day precipitation across the domain. This means that the maximum five day precipitation will increase even in regions where precipitation will decrease. This fits with the change we see in the number of precipitation days. It is interesting to note that the largest increase in maximum five day precipitation is in the northeast, a region not associated with precipitation increase. The PDFs are shifted to the right (wetter) at higher SWLs reflecting the increase in maximum five day precipitation, but they are also getting wider showing that there still are regions with low maximum five day precipitation. There are clear differences between the high and low resolution simulations. The high resolution simulations give a higher probability for larger maximum five day precipitation. At SWL6 the high resolution simulation resembles what is given by ERA-Interim in the control period.

South-East Asia

The changes in precipitation are difficult to assess because the signal is weak at SWL2 and at SWL4 there are only two simulations available (and only one at SWL6). With that caveat we find that the general increase in precipitation at SWL2 is replaced by a pattern of decreasing precipitation in the south and the north and increasing precipitation in the centre of the domain. This implies a southward shift of the region of large precipitation in the central-eastern part of the domain. Nevertheless the overall distribution of precipitation remains the same, but with a shift towards higher precipitation amounts.

The number of days with precipitation over 10 mm changes in the same way as the mean precipitation: more where precipitation increases and less where precipitation decreases; this mostly effects the regions with a large number of days above 10 mm precipitation. The probability of more than 60 days of more than 10 mm precipitation will be reduced in a warmer climate.

The maximum five day precipitation changes in a more random way, at SWL2 there is about as much increase as decrease (Fig 20). It is clear, however, that the maximum five day precipitation will increase with higher SWLs. At SWL6 the IPSL-driven simulations show increasing five day precipitation across most of the domain. This means that the maximum five day precipitation will increase even in regions where precipitation will decrease. The largest maximum five day precipitation will increase from around 1000 mm at SWL2 to around 1800mm at SWL6. The PDFs are also getting wider showing that there still are regions with low maximum five day precipitation. There are clear differences between the high and low resolution simulations. The high resolution simulations give a higher probability for larger maximum five day precipitation.

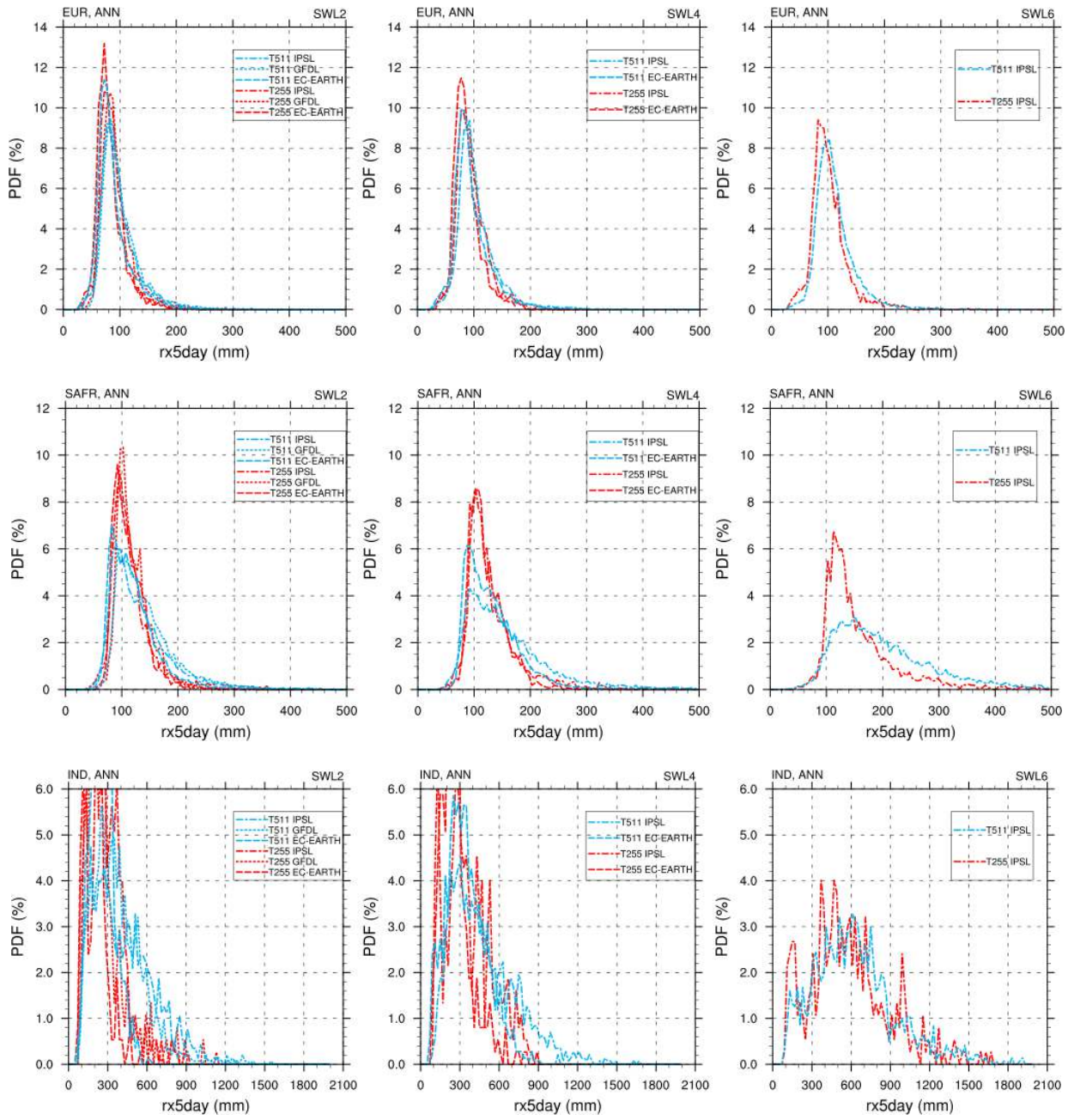

Figure 20: PDF of the maximum five day precipitation (mm, rx5day) over Europe (top), southern Africa (middle) and South-East Asia (bottom) for high resolution (T511, blue lines) and low resolution simulations (T255, red lines) for SWL2 (left), SWL4 (middle) and SWL6 (right).

6 Conclusions

In this report we compare a subset of CMIP5 models against new high-resolution downscalings that were forced with SST and SIC from these CMIP5 models. Compared to CMIP5 models, the higher resolution of the AGCMs used in HELIX does result in a better representation of the orography and consequently colder temperatures and larger precipitation amounts over mountainous areas which allows for a better representation of extremes. These features of higher resolution are not limited to the present-day climate but are also present in climate projections of the future.

For the mean temperature the overall spatial distribution agrees well between CMIP5 models and the new HELIX downscalings. The magnitude and spatial pattern of the mean temperature change at various SWLs is similar in the set of CMIP5 and the new HELIX simulations. Similar conclusions can also be drawn for temperature extremes, although the variability arising from different forcings appears to be larger for temperature extremes than for the mean temperature, especially when looking at the different SWLs.

The limited set of temperature extremes indices presented here also indicate similar consistency between the CMIP and HELIX simulations with the primary benefit being the better spatial representation, particularly in regions of varying topography and coastlines. In future work it is intended to expand the range of temperature extremes indices considered to look at measures of minimum temperature and variability, and also indices representing aspects of heat waves and growing season.

The magnitude and pattern of the mean precipitation are similar in the set of CMIP5 and the HELIX downscalings. However, measures for precipitation extremes reveal differences between low resolution CMIP5 and high resolution HELIX models, particularly for threshold based indices such as r20mm. The higher resolution increases the frequency of occurrence for high precipitation events which results e.g. in more days with high precipitation.

While the changes in mean precipitation in the SWLs compared to the present-day climate are rather similar in the CMIP5 and the HELIX models, the changes in the precipitation extremes show a different picture. While CMIP5 models may show an increase of rainy days or maximum 5-day precipitation amounts in the HELIX target regions, the HELIX models may show a decrease of the same index, or vice versa. Given the fact that the HELIX downscalings are done with SST and SIC from the same subset of CMIP5 variables, we can thus conclude that the response of precipitation extremes to a changing climate clearly depends on the resolution of the atmospheric model.

The differences that were obtained by comparing low resolution CMIP5 models with the new high resolution downscalings may not only be caused by the higher resolution of the HELIX models but there could also be other causes related to model developments. For example the EC-EARTH3 has a new microphysics scheme that also may contribute to changes in precipitation (HadGEM3 also incorporates new physics compared with HadGEM2). Some of the new high-res simulations for EC-EARTH were thus repeated with lower spatial resolution, the EC-EARTH3 model being the same in both cases. The results from this comparison confirm the earlier findings of the comparison against the subset of CMIP5 models: the higher resolution has limited impact on the representation of the temperature but a larger impact on precipitation, in particular the representation of high precipitation events. Compared with reanalyses we find that the new HELIX simulations with higher horizontal resolution are in better agreement than the subset of CMIP5 models.

Acknowledgements

The EC-EARTH3 simulations were performed on resources provided by the Swedish National Infrastructure for Computing (SNIC) at PDC.

References

Berckmans, J., Woollings, T., Demory, M.-E., Vidale, P.-L. and Roberts, M. (2013), Atmospheric blocking in a high resolution climate model: influences of mean state, orography and eddy forcing. Atmos. Sci. Lett., 14: 34–40. doi:10.1002/asl2.412

Chan S. C., Elizabeth J. Kendon, Hayley J. Fowler, Stephen Blenkinsop, Christopher A. T. Ferro, David B. Stephenson, 2013: Does increasing the spatial resolution of a regional climate model improve the simulated daily precipitation? Climate Dynamics, 41, 1475–1495.

Dawson A., T. N. Palmer. 2014: Simulating weather regimes: impact of model resolution and stochastic parameterization. Climate Dynamics., 44, 2177–2193.

Dee, D.P., Uppala, S.M., Simmons, A.J., Berrisford, P. Poli, P., Kobayashi, S., Andrae, U., Balmaseda, M. A., Balsamo, G., Bauer, P., Bechtold, P., Beljaars, A.C.M., van de Berg, L., Bidlot, J., Bormann, N., Delsol, C., Dragani, R., Fuentes, M., Geer, A. J., Haimberger, L., Healy, S. B., Hersbach, H., Hólm, E.V., Isaksen, L., Kållberg, P., Köhler, M., Matricardi, M., McNally, A.P., Monge-Sanz, B.M., Morcrette, J.-J., Park, B.-K. Peubey, C., de Rosnay, P., Tavolato, C., Thépaut, J.-N., and Vitart, F., 2011: The ERA-Interim reanalysis: configuration and performance of the data assimilation system, Quart. J. Roy. Met. Soc., 137, 656, 553–597

Demory, M. E., Vidale, P. L., Roberts, M. J., Berrisford, P., Strachan, J., Schiemann, R., & Mizielinski, M. S. (2014). The role of horizontal resolution in simulating drivers of the global hydrological cycle. Climate Dynamics, 42(7-8), 2201-2225.

Diamantakis, M and Flemming, J, 2013: Global mass fixer algorithms for conservative tracer transport in the ECMWF model. ECMWF TM 713, Available on-line: http://www.ecmwf.int/en/elibrary/9055-global-mass-fixer-algorithms-conservative-tracer-transport-ecmwf-model

Forbes, R, Tompkins, AM, and Untch, A, 2011: A new prognostic bulk microphysics scheme for the IFS. ECMWF TM 649. Available on-line: http://www.ecmwf.int/en/elibrary/9441-new-prognostic-bulk-microphysics-scheme-ifs

Gohar LK, Bernie D and Lowe JA. 2014. Evaluation of timing of SWLs from existing models. Report D2.1 to the HELIX programme

Hazeleger, W. et al., 2012: EC-Earth V2.2: description and validation of a new seamless earth system prediction model. Clim. Dyn., 39, 2611-2629. doi:10.1007/s00382-011-1228-5

Hazeleger W., V. Guemas, B. Wouters, S. Corti, I. Andreu–Burillo, F. J. Doblas–Reyes, K. Wyser, and M. Caian 2013: Multiyear climate predictions using two initialization strategies. Geophys. Res. Let., 40, 1794–1798. doi: 10.1002/grl.50355

Haylock, M.R., Hofstra, N., Klein Tank, A.M.G., Klok, E.J., Jones, P.D. and New, M., 2008: A European daily high-resolution gridded data set of surface temperature and precipitation for 1950–2006. J. Geophys. Res., 113, 0119, doi:10.1029/2008JD010201

Hewitt, H. T., Copsey, D., Culverwell, I. D., Harris, C. M., Hill, R. S. R., Keen, A. B., McLaren, A. J., and Hunke, E. C.: Design and implementation of the infrastructure of HadGEM3: the next-generation Met Office climate modelling system, Geosci. Model Dev., 4, 223-253, doi:10.5194/gmd-4-223-2011, 2011.

Jung T., M. J. Miller, T. N. Palmer, P. Towers, N. Wedi, D. Achuthavarier, J. M. Adams, E. L. Altshuler, B. A. Cash, J. L. Kinter III, L. Marx, C. Stan, and K. I. Hodges, 2012: High-Resolution Global Climate Simulations with the ECMWF Model in Project Athena: Experimental Design, Model Climate, and Seasonal Forecast Skill. J. Climate, 25, 3155–3172.

Knight, J., et al. (2014), Predictions of climate several years ahead using an improved decadal prediction system, J. Clim., 27, 7550–7567, doi:10.1175/JCLI-D-14-00069.1.

MacLachlan, C., et al. (2014), Global Seasonal forecast system version 5 (GloSea5): A high-resolution seasonal forecast system, Q. J. R. Meteorol. Soc., 141, 1072–1084, doi:10.1002/qj.2396.

G. M. Martin, Bellouin, N., Collins, W. J., Culverwell, I. D., Halloran, P. R., Hardiman, S. C., Hinton, T. J., Jones, C. D., McDonald, R. E., McLaren, A. J., O'Connor, F. M., Roberts, M. J., Rodriguez, J. M., Woodward, S., Best, M. J., Brooks, M. E., Brown, A. R., Butchart, N., Dearden, C., Derbyshire, S. H., Dharssi, I., Doutriaux-Boucher, M., Edwards, J. M., Falloon, P. D., Gedney, N., Gray, L. J., Hewitt, H. T., Hobson, M., Huddleston, M. R., Hughes, J., Ineson, S., Ingram, W. J., James, P. M., Johns, T. C., Johnson, C. E., Jones, A., Jones, C. P., Joshi, M. M., Keen, A. B., Liddicoat, S., Lock, A. P., Maidens, A. V., Manners, J. C., Milton, S. F., Rae, J. G. L., Ridley, J. K., Sellar, A., Senior, C. A., Totterdell, I. J., Verhoef, A., Vidale, P. L., and Wiltshire, A.: The HadGEM2 family of Met Office Unified Model climate configurations, Geosci. Model Dev., 4, 723-757, doi:10.5194/gmd-4-723-2011, 2011.

Molteni, F, Stockdale, T, M. Balmaseda, A, Balsamo, G, Buizza, R, Ferranti, L, Magnusson, L, Mogensen, K, Palmer, TN, and Vitart, F, 2011: The new ECMWF seasonal forecast system (System 4). ECMWF TM 656. Available on-line: http://www.ecmwf.int/en/elibrary/11209-new-ecmwf-seasonal-forecast-system-system-4

Moss RH, Edmonds JA, Hibbard KA, Manning MR, Rose SK et al (2010) The next generation of scenarios for climate change research and assessment. Nature 463:747–756

Morcrette, J.-J., Barker, H., Cole, J., Iacono, M. and Pincus, R., 2008: Impact of a new radiation package, mcrad, in the ECMWF integrated forecasting system. Mon. Wea. Rev., 136, 4773-4798.

Murakami, H., G. Vecchi, S. Underwood, T. Delworth, A. Wittenberg, W. Anderson, J. Chen, R. Gudgel, L. Harris, S. Lin, and F. Zeng, 2015: Simulation and Prediction of Category 4 and 5 Hurricanes in the High-Resolution GFDL HiFLOR Coupled Climate Model. J. Climate, 28, 9058–9079, doi: 10.1175/JCLI-D-15-0216.1.

Riahi, K., Rao, S., Krey, V. et al. Climatic Change (2011) 109: 33. doi:10.1007/s10584-011-0149-y

Senior, C. A., et al. (2016), Idealized climate change simulations with a high-resolution physical model: HadGEM3-GC2, J. Adv. Model. Earth Syst., 8, 813–830, doi:10.1002/2015MS000614.

Van Haren, R., Haarsma, R. J., Van Oldenborgh, G. J., & Hazeleger, W. (2015). Resolution dependence of European precipitation in a state-of-the-art atmospheric general circulation model. Journal of Climate, 28(13), 5134-5149.

Walters, D. N., Brooks, M. E., Boutle, I. A., Melvin, T. R. O., Stratton, R. A., Bushell, A. C., Copsey, D., Earnshaw, P. E., Gross,M. S., Hardiman, S. C., Harris, C. M., Heming, J. T., Klingaman, N. P., Levine, R. C., Manners, J., Martin, G. M., Milton, S. F., Mittermaier, M. P., Morcrette, C. J., Riddick, T. C., Roberts, M. J., Selwood, P. M., Tennant, W.J., Vidale, P.-L., Wilkinson, J. M., Wood, N., Woolnough, S. J., and Xavier, P. K.: The Met Office Unified Model Global Atmosphere 6.0 and JULES Global Land 6.0, submitted to Geoscientific Model Development, 2016

Winton, M., W. G. Anderson, T. L. Delworth, S. M. Griffies, W. J. Hurlin, and A. Rosati (2014), Has coarse ocean resolution biased simulations of transient climate sensitivity?, Geophys. Res. Lett., 41, 8522–8529.

Wood, N., Staniforth, A., White, A., Allen, T., Diamantakis, M., Gross, M., Melvin, T., Smith, C., Vosper, S., Zerroukat, M. and Thuburn, J. (2014), An inherently mass-conserving semi-implicit semi-Lagrangian discretization of the deep-atmosphere global non-hydrostatic equations. Q.J.R. Meteorol. Soc., 140: 1505–1520. doi:10.1002/qj.2235

Zhang, X, L. Alexander, G.C. Hegerl, P.D. Jones, A. Klein-Tank, T.C. Peterson, B. Trewin and F. Zwiers (2011): Indices for Monitoring Changes in Extremes based on Daily Temperature and Precipitation Data. WIREs Clim Change 2011. doi: 10.1002/wcc.147